ADVANCES IN ATMOSPHERIC SCIENCES, VOL. 33, AUGUST 2016, 969–978

Evaluation of a Micro-scale Wind Model's Performance over Realistic Building Clusters Using Wind Tunnel Experiments

Ning ZHANG*[1], Yunsong DU[1,2], Shiguang MIAO[3], and Xiaoyi FANG[4]

[1]*Institute for Climate and Global Change Research and School of Atmospheric Sciences, Nanjing University, Nanjing* 210093
[2]*Sichuan Environmental Monitoring Center, Chengdu* 610091
[3]*Institute of Urban Meteorology, China Meteorological Administration, Beijing* 100089
[4]*Beijing Municipal Climate Center, Beijing* 100089

(Received 7 January 2016; revised 16 April 2016; accepted 18 April 2016)

ABSTRACT

The simulation performance over complex building clusters of a wind simulation model (Wind Information Field Fast Analysis model, WIFFA) in a micro-scale air pollutant dispersion model system (Urban Microscale Air Pollution dispersion Simulation model, UMAPS) is evaluated using various wind tunnel experimental data including the CEDVAL (Compilation of Experimental Data for Validation of Micro-Scale Dispersion Models) wind tunnel experiment data and the NJU-FZ experiment data (Nanjing University-Fang Zhuang neighborhood wind tunnel experiment data). The results show that the wind model can reproduce the vortexes triggered by urban buildings well, and the flow patterns in urban street canyons and building clusters can also be represented. Due to the complex shapes of buildings and their distributions, the simulation deviations/discrepancies from the measurements are usually caused by the simplification of the building shapes and the determination of the key zone sizes. The computational efficiencies of different cases are also discussed in this paper. The model has a high computational efficiency compared to traditional numerical models that solve the Navier–Stokes equations, and can produce very high-resolution (1–5 m) wind fields of a complex neighborhood scale urban building canopy (~ 1 km ×1 km) in less than 3 min when run on a personal computer.

Key words: numerical model, urban wind field, wind tunnel experiment data, emergency response model

Citation: Zhang, N., Y. S. Du, S. G. Miao, and X. Y. Fang, 2016: Evaluation of a micro-scale wind model's performance over realistic building clusters using wind tunnel experiments. *Adv. Atmos. Sci.*, **33**(8), 969–978, doi: 10.1007/s00376-016-5273-1.

1. Introduction

Cities are usually composed of complex geometric units such as street canyons, roads and buildings, and the urban climate is strongly affected by the geometries and materials making up urban canyons (Arnfield, 2003). Knowledge of the meteorological processes of urban canyons is important to understand the microscale climate/environment within urban canopies, as well as to understand the full-scale urban climate. The wind field is a key property not only affecting the energy and moisture advection and the exchange of energy/water between the urban surface and the atmosphere, but also linking environmental issues such as energy consumption, ventilation in buildings and dispersion of air pollutants, as well as human comfort and safety (Vardoulakis et al., 2003).

Wind fields and concentrations of air pollutants in urban street canyons or urban canopies have been widely investigated using wind tunnel experiments and numerical simulations; several field experiments have also been carried out for this purpose (Rotach et al., 2005; Hu et al., 2016). A significant amount of research has focused on the complicated flow characteristics around buildings and within urban street canyons, due to its critical role in the dispersion of air pollutants in urban environments.

The wind field around a building can be characterized by several key zones, including the upwind cavity, lee-side cavity, and rooftop recirculation zone. The wind patterns become more complicated between two rows of buildings (street canyons); Oke (1988) classified the wind flow in a street canyon into three types: isolated roughness flow, wake interface flow, and skimming flow. More complex structures have been found using numerical simulations (Xie et al., 2008; Li et al., 2010; Hertwig et al., 2012; Michioka et al., 2013), physical experiments (Ahmad et al., 2005; Chang et al., 2013; Marciotto and Fisch, 2013), and *in-situ* observations (Eliasson et al., 2006; Offerle et al., 2007; Fujiwara et al., 2011; Claus et al., 2012; Wood et al., 2013).

Computational fluid dynamical (CFD) models, including

* Corresponding author: Ning ZHANG
Email: ningzhang@nju.edu.cn

large-eddy simulation (LES) models and Reynolds-Averaged Navier–Stokes simulations, are widely used to simulate urban wind fields (Xie et al., 2008; Li et al., 2010; Ashie and Kono, 2011; Hertwig et al., 2012; Michioka et al., 2013). Wyszogrodzki et al. (2012) coupled an LES model with the mesoscale Weather Research and Forecasting model to obtain fine-scale wind field predictions over an urban area. However, such models are usually expensive and require significant CPU time for city-scale simulations (Ashie and Kono, 2011). Several fast models (Singh et al., 2008; Kochanski et al., 2015; Salem et al., 2015; Zhang et al., 2016) have been developed to simulate the wind flow/air dispersion in building clusters, with relatively lower accuracy and less CPU time, for emergency response conditions on the urban neighborhood scale. Some of these models have been implemented with weather forecasting models for neighborhood-scale urban environment services (Kochanski et al., 2015).

Zhang et al. (2016) introduced the Urban Microscale Air Pollution dispersion Simulation model (UMAPS), which includes a diagnostic model (Wind Information Field Fast Analysis model, WIFFA) to simulate wind fields around urban buildings and a Random Walk air pollutant dispersion Model (Nanjing University random walk dispersion model, NJU-RWM) to simulate the pollutant transport in urban canopies. The wind field model (WIFFA) is composed of two parts: an interpolation model to obtain the first-guess fields of different zones around a building or street canyon, and a mass conservation wind model to obtain the detailed wind field over the entire simulation domain. The performance of WIFFA is fundamental to the simulation performance of the entire system, and it is important to know how well such a simplified model can represent the wind fields over complex and real building clusters.

This paper expands upon the work of Zhang et al. (2016) to evaluate the performance of the wind model (WIFFA) against wind tunnel experimental data, as the simulation of wind fields is fundamental for air pollution dispersion simulation in urban areas.

2. Wind tunnel and numerical experiment settings

2.1. *CEDVAL wind tunnel experiments (B1-4)*

Two wind tunnel datasets were used for the evaluations in this paper. The first was the B1-4 experiment in the CEDVAL database. CEDVAL is a wind tunnel dataset for model evaluations of flow patterns and air pollutant dispersion around buildings (Compilation of Experimental Data for Validation of Microscale Dispersion Models, http://www.mi.uni-hamburg.de/CEDVAL_Validation_Data.427.0.html). The B1-4 experiment in the CEDVAL database measures the wind fields around four square-ring buildings, two of them with slanted roofs. The building model height (H_s) is 0.06 m, and the length and width are both $4.17H_s$ (without the roofs). The physical scale factor is 1 : 200; therefore, the real building height would be 12 m. The distribution of the buildings is shown in Fig. 1. The measurements were taken under neutral conditions, and wind fields in six sections were observed, including two horizontal sections at $z = 0.5H_s$ and $z = 0.83H_s$, and four vertical sections at $y = -2.58H_s$, $y = -1.0H_s$, $y = 2.0H_s$ and $y = 3.58H_s$, marked as A, B, C and D in Fig. 1. The inlet flow in the experiment was set as a power-law profile, $u(z) = U_{\rm ref} \times (z/100.0)^{0.22}$; the reference height was 100.0 m, the reference wind speed ($U_{\rm ref}$) was 6.0 m s^{-1}, and the power coefficient was 0.22.

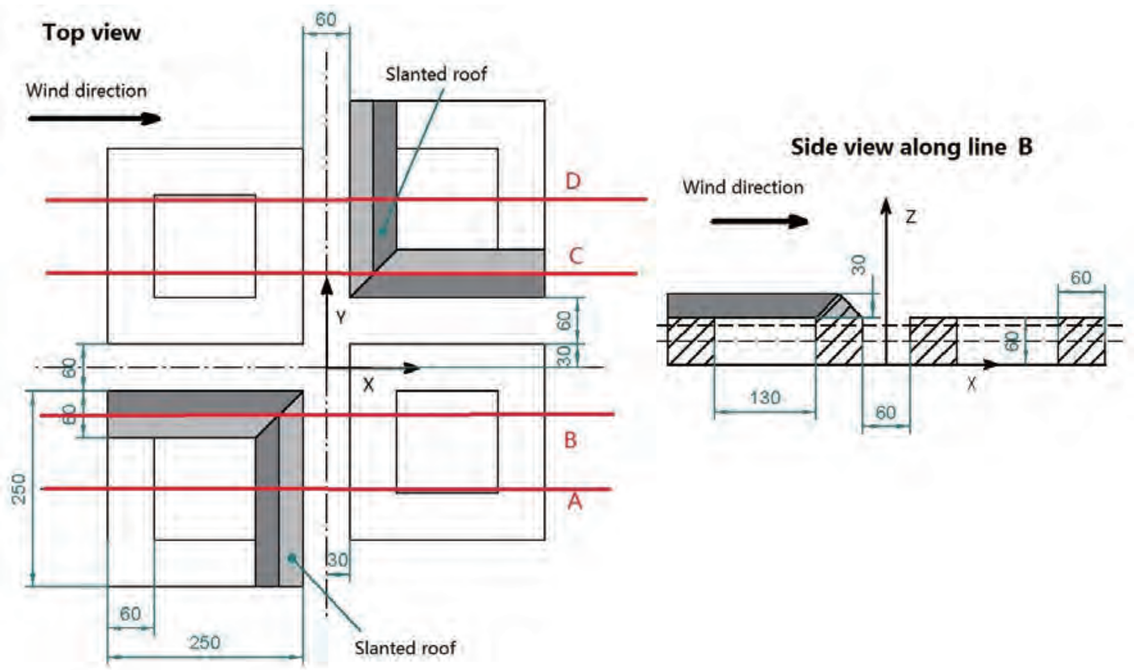

Fig. 1. The wind tunnel physical model for the CEDVAL B1-4 experiment (from the CEDVAL database).

In the numerical simulations, the building shape was calculated using the physical scale factor, the building length/width/height (without a roof) was 50 m/50 m/12 m, the roof top height was 18 m, and the street canyon width was 12 m. The simulation domain was set to $X \times Y \times Z =$ 400 m : 200 m : 100 m, and both the horizontal and vertical resolutions were 1 m. The inlet flow was set following the x-coordinate, and the wind profile was the same as in the wind tunnel experimental setting.

2.2. *NJU-FZ wind tunnel experiments*

The second database used in this paper was the Nanjing University-Fang Zhuang neighborhood (NJU-FZ) wind tunnel experiment dataset. The wind tunnel experiments were conducted in the Nanjing University Environmental Wind Tunnel to simulate wind fields and air pollutant dispersion in a real neighborhood in Beijing (Ouyang et al., 2003). The neighborhood size was 500 m $\times$ 700 m and included 30 buildings; the average building height was 32.4 m and ranged from 4 m to 78 m. The model physical scale factor was 1 : 250. The wind fields were measured under two wind directions and two reference wind speeds, and the inlet flow was set as a power profile, as shown in Table 1. Three wind speed profiles were observed for different wind direction experiments at different locations, as shown in Fig. 2.

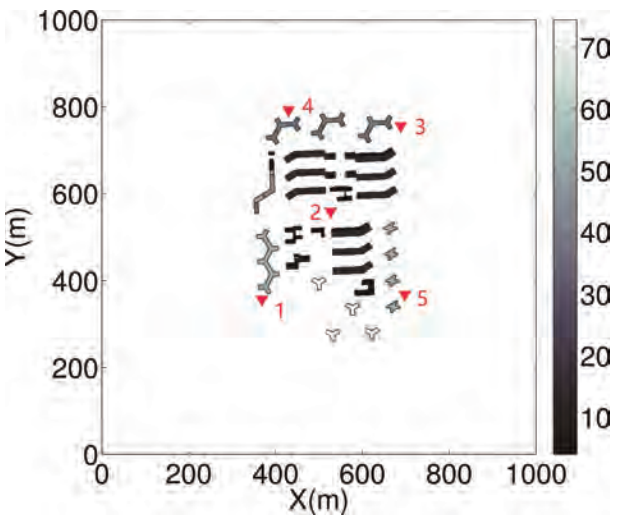

Fig. 2. The building distribution and measurement locations for the FZ wind tunnel experiments (triangles represent the vertical profile measurement locations; the numbers 1–3 indicate the southwest experiments; and 4, 2 and 5 the northwest experiments).

Locations 1, 2 and 3 are for the southwest wind experiments and locations 2, 4 and 5 are for the northwest wind experiments. The wind profiles were measured at 14 points and the vertical spatial distances varied with height. The numerical simulation domain for the real neighborhood experiments was set to 1000 m $\times$ 1000 m $\times$ 200 m. The horizontal and vertical resolutions were 5 m and 2 m, respectively. The inlet wind flows were set to be same as the wind tunnel experiments.

The same evaluation methods as used in Zhang et al. (2016) are used in the present study, and the following statistical parameters are employed: the mean value (MN); the mean error between simulations and observations (E), the relative simulation error (RE); the root-mean-square error (RMSE); the normalized RMSE (NMSE), the correlation coefficient (R), and the factor of two of observations (FAC2). The definitions are as follows:

$$\mathrm{MN} = \overline{X_i}(i = \mathrm{o}, \mathrm{p})\ ;$$
$$E = X_\mathrm{o} - X_\mathrm{p}\ ;$$
$$\mathrm{RE} = |\overline{X_\mathrm{o}} - \overline{X_\mathrm{p}}| / \overline{X_\mathrm{o}}\ ;$$
$$\mathrm{RMSE} = \sqrt{\overline{(X_\mathrm{o} - X_\mathrm{p})^2}}\ ;$$
$$\mathrm{NMSE} = \frac{\overline{(X_\mathrm{o} - X_\mathrm{p})^2}}{\overline{X_\mathrm{o}}\,\overline{X_\mathrm{p}}}\ ;$$
$$R = \frac{\overline{(X_\mathrm{o} - \overline{X_\mathrm{o}})(X_\mathrm{p} - \overline{X_\mathrm{p}})}}{\sigma_{X_\mathrm{o}}\sigma_{X_\mathrm{p}}}\ ;$$
$$\mathrm{FAC2} = \frac{\mathrm{N}(0.5 \leqslant X_\mathrm{p}/X_\mathrm{o} \leqslant 2.0)}{\mathrm{N}}\ ,$$

where X_o is the wind tunnel–measured value and X_p is the respective numerically simulated one.

3. Results

3.1. *The CEDVAL B1-4 experiment*

The numerical simulation results were bilinearly interpolated at the wind tunnel measurement locations to evaluate the model performance. Figure 3 compares the horizontal wind fields in the $z/H = 0$ and $z/H = 0.83$ sections for the wind tunnel observations and the numerical simulations. The results show that complex flow patterns occurred due to the building shapes and distributions. Additionally, vortex patterns appeared at both the exits of the y-direction street canyon and the cross sections of the canyons. The model can capture the flow patterns well; the REs in the $z/H = 0.5$ and $z/H = 0.83$

Table 1. The settings of the FZ wind tunnel experiments.

Experiment name	Wind direction	Reference wind speed (m s^{-1})	Reference height (m)	The power exponent
FZ-A	Southwest	1.22	37.5	0.10
FZ-B	Southwest	2.88	37.5	0.10
FZ-C	Northwest	1.22	37.5	0.10
FZ-D	Northwest	2.88	37.5	0.10

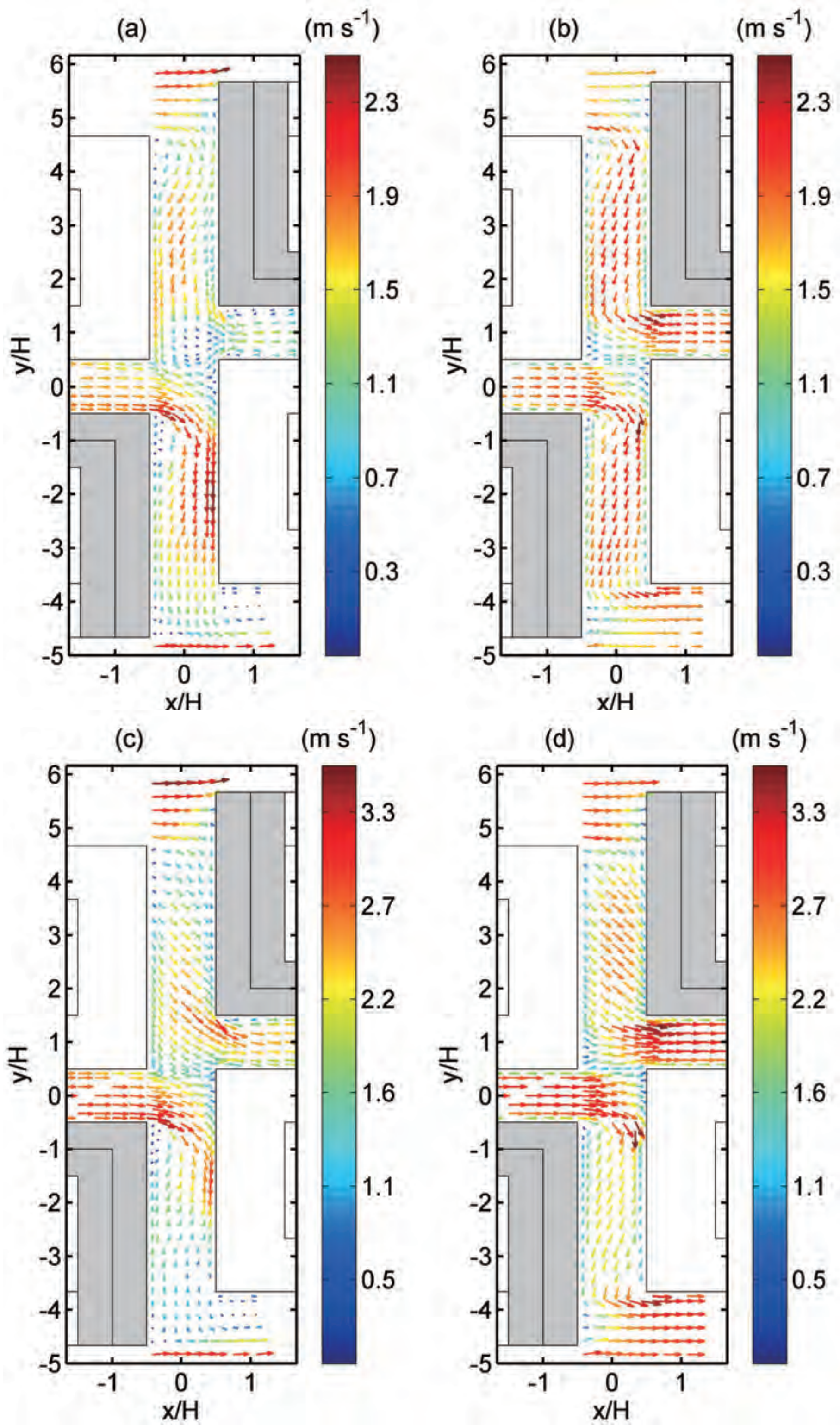

Fig. 3. The horizontal wind fields in different sections in the CEVAL B1-4 experiments: (a) observed and (b) simulated results at $z/H = 0.50$; and (c) observed and (d) simulated results at $z/H = 0.83$.

sections are 1.8% and 27.8%, respectively, and the FAC2s are greater than 85%. The model overestimated the wind speed at $z/H = 0.83$, and the mean bias is 0.51 m s^{-1}. This error results primarily from the overestimation of the wind speed near the y-direction orientated street canyon; this also causes the low R between the observations and simulations, as shown in Table 2.

The horizontal profiles of normalized wind velocities

Table 2. Comparison of observations and simulations in different sections in the CEDVAL B1-4 experiment.

	NUM	MN_{tunnel}	MN_{model}	RE	NMSE	R	FAC2
$z/H = 0.5$	412	1.66	1.69	1.8%	0.13	43.3%	85.4%
$z/H = 0.83$	460	1.83	2.34	27.8%	0.17	48.7%	88.9%
$y/H = -2.58$	193	1.51	3.04	100.0%	0.63	83.2%	39.9%
$y/H = -1.0$	169	2.05	3.07	49.4%	0.23	95.2%	63.3%
$y/H = 2.0$	169	2.17	3.01	38.7%	0.14	92.4%	80.5%
$y/H = 3.58$	187	1.89	3.06	61.9%	0.35	75.4%	64.7%

NUM: Measure point number at each section

($u/U_{ref}, v/U_{ref}$) and normalized wind speed ($U/U_{ref}, U = \sqrt{u^2 + v^2}$) at $x/H = 0.0$ at different levels were compared, as shown in Fig. 4. The simulation error at $z/H = 0.50$ results from the overestimation of u between $y/H = 0.0$ and 1.0; the overestimations of the u value between $y/H = -1.0$ and 1.0 and the overestimations of the v value at $y/H > 2.0$ and $y/H < -2.0$ contribute to the overestimation of the total wind speed in the $z/H = 0.83$ section. As shown in Zhang et al. (2016), the first-guess part of WIFFA usually overestimates the horizontal wind speed in the lateral wall zone around a bulk building. In this experiment, the horizontal wind speed in the street canyon between the downward buildings is overestimated in the first-guess part as well, and then the following mass conversation formula (MCF) model calculates a higher wind speed in the y-orientated street canyon to meet the restriction of the equation of continuity.

The observed and simulated vertical sections are shown in Fig. 5. A clockwise vortex appears in vertical sections A, C and D in both the wind tunnel experiment and the numerical simulations. The vortex circulation center appears at 1.25H, 0.6H and 0.8H in sections A, C and D; while the respective simulated location is at approximately 0.9H. The clockwise vortex also appears in section B in the numerical simulations, because the wind field in this section is also calculated as the "skimming flow type"; while the vortex is not measured in the wind tunnel experiments. Because the wind speed in the street canyon is relatively weak, the R values between the experiment and simulations can also be above 0.75 for all sections. The slanted roofs also trigger cavity vortexes in section A and D; however, this is not represented well in the model simulations. The model overestimated the wind speed in all vertical sections. The largest simulation error oc-

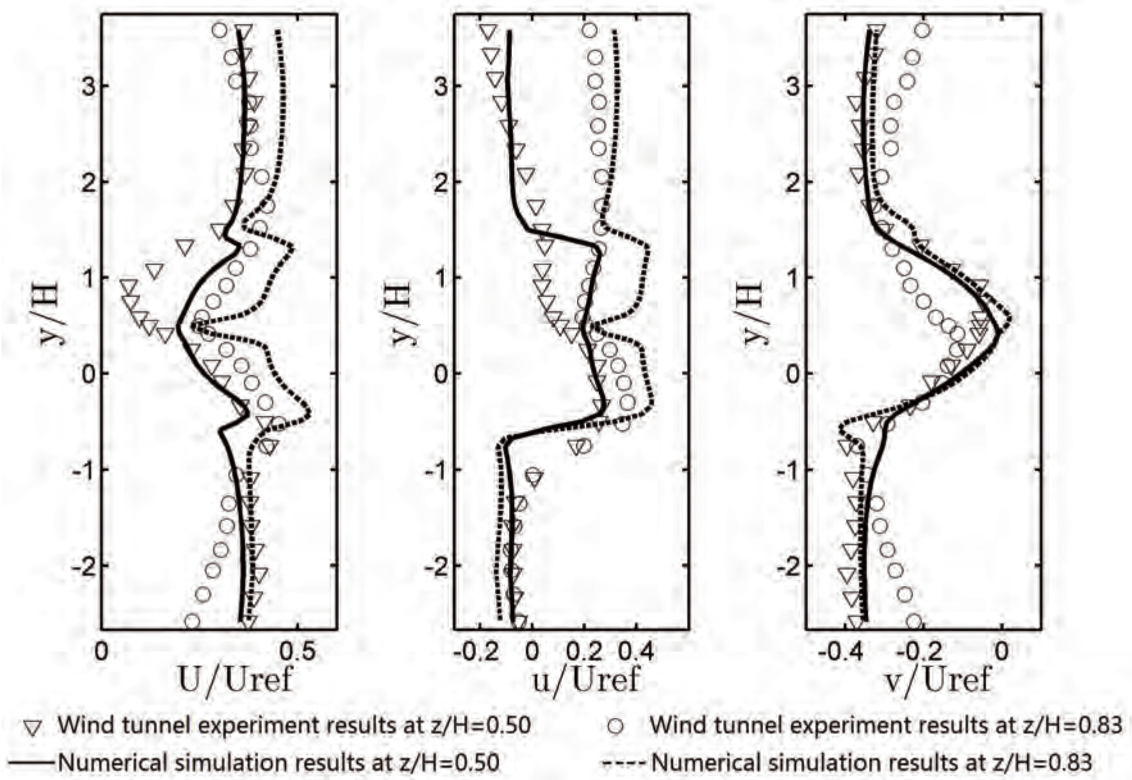

Fig. 4. Wind speeds and velocities along $x/H = 0.0$ in the $z/H = 0.5$ and $z/H = 0.83$ sections.

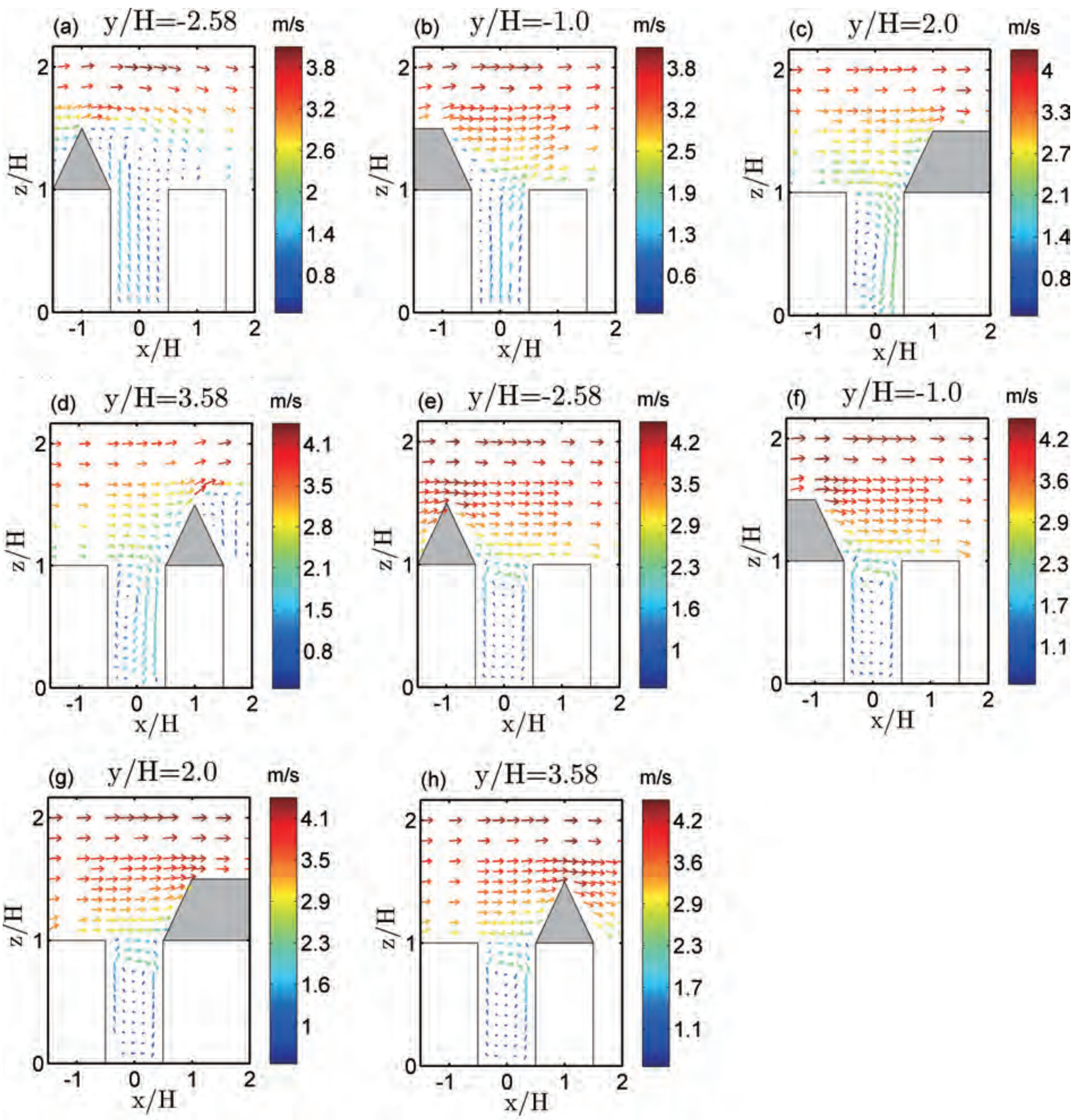

Fig. 5. The (a–d) observed and (e–h) simulated wind fields in different vertical sections (sections A, B, C and D, as shown in Fig. 1) in the CEDVAL B1-4 experiment.

curred in section A, with RE = 100%, NMSE = 49.4%, and FAC2 = 39.9%.

3.2. *The real neighborhood experiments*

Figure 6 illustrates the simulated wind fields at a height of 5 m under different wind directions. Due to blocking by buildings, the wind speed is weak before the upwind walls of buildings and vortexes appear behind the buildings. The channeling effect is also captured by the model; the wind speed between tall buildings may be greater than the incoming wind speed. Longer buildings triggered larger cavities and caused larger weak wind areas.

The simulated vertical wind speed profiles were compared with the observations, as shown in Figs. 7 and 8, revealing the simulations agreed well with the observations. Vertical profiles at different locations show different characteristics under different inlet wind directions, and the profiles at the same positions are similar with different inlet wind speeds. In the southwest wind experiments, the wind speeds at location 1 show a power-law profile above 50 m; while for levels under 50 m, the wind speed first increases with height from the ground, reaches a peak at a height of approximately 35 m, and then decreases with increasing height. Location 2 is in the open-space of the neighborhood, and the wind

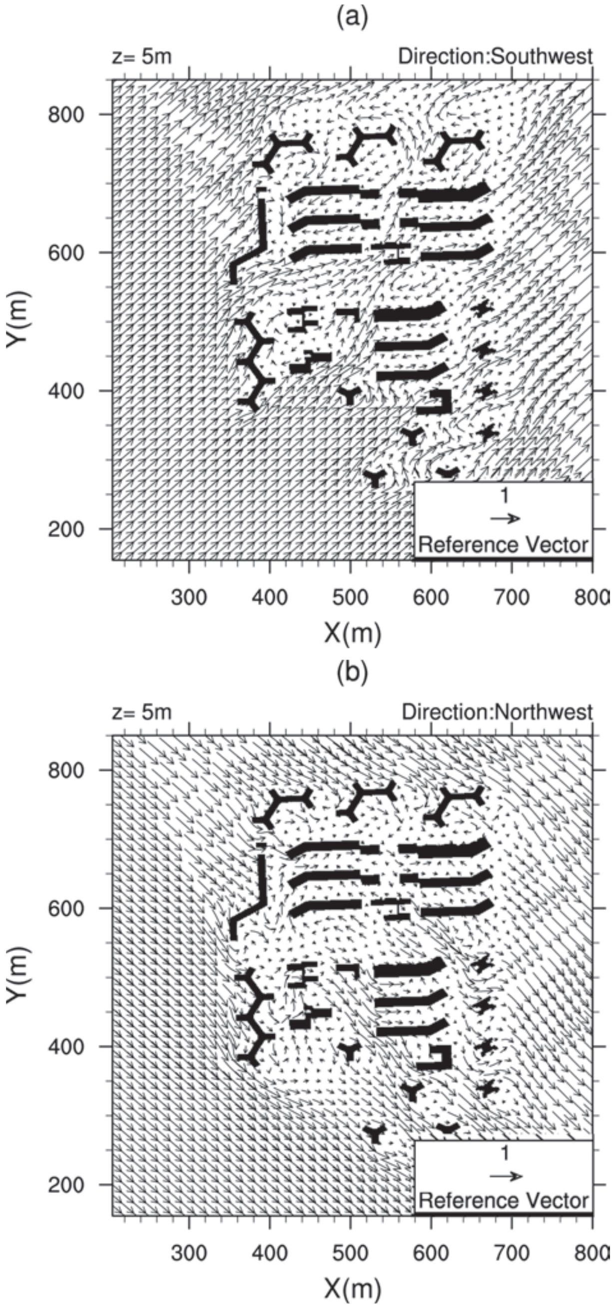

Fig. 6. The simulated wind fields in a real neighborhood at a height of 5 m under different wind directions with an incoming wind speed of 1.22 m s^{-1}: (a) southwest wind; (b) northwest wind.

profiles at this position resemble a power-law. Location 3 is in a cavity behind a building, and therefore the wind speed under 40 m is very low but increases dramatically above 40 m. In the northwest experiments, location 4 is located before the building clusters, and the wind profiles are not affected by the buildings at this position. Locations 2 and 5 are now on the downwind side of the buildings, and the wind speed is low at the lower levels and increases dramatically at the upper levels. The largest RMSE occurred at location 5 with a value of 0.56 m s^{-1}, due to the simulation of the skimming flow patterns above the building roofs.

3.3. *Computational efficiency*

Computational efficiency is important for emergency response models. In this paper, the model was compiled using an Intel Fortran Compiler (version 11.), and all numerical simulations were run on a Linux PC with an AMD (Advanced Micro Devices company) 2.66 GHz CPU and 8 G of memory. The CPU time-cost is listed in Table 3. All simulations cost less than 4 min; and low-resolution runs can save additional CPU time. Another factor affecting the computational efficiency is the convergence of the MCF model; all experiments in this paper used the maximum step number of the iteration in the MCF model. The CPU time-cost reduces significantly when the first-guess wind field has good convergent characteristics. The current experiments show that the number of buildings included in the simulation does not influence the computational efficiency.

The computational efficiency of the current model is much higher than previous simulations by Zhang et al. (2006) with an LES model, which cost 3–5 h for a 30-min FZ-A/FZ-B simulation on the same PC platform. The simulation accuracy of WIFFA is less than that of the LES model due to the lack of physical progress description (details are not discussed in this paper), but the comparisons between the numerical simulations and wind tunnel experiments can also prove that UMAPS is able to output relatively accurate wind fields, even when only using an empirical diagnosis first-guess method and a simple MCF model. At the same time, the computational efficiency is highly improved compared to the CFD method, because it does solve the full complex Navier–Stokes equation. WIFFA is a good trade-off tool for urgent urban air pollution episodes, when both computational efficiency and the simulation accuracy should be considered.

4. Summary

The diagnostic wind field model (WIFFA) is an important part of the micro-scale air pollutant model system (UMAPS) because it supplies wind field information to the subsequent air pollutant dispersion model. WIFFA is composed of two parts: an interpolation model to obtain the first-guess fields of different zones around a building or street canyon, and a mass conservation wind model to obtain a detailed wind field over the entire simulation domain. The model simulates the wind fields around a complex building with a very simple and fast method; therefore, it is important to understand how well the model works for further development.

The simulation performance over complex building clusters with WIFFA was evaluated using different wind tunnel experimental data, including CEDVAL wind tunnel experiment data and FZ wind tunnel experiment data. The results show that the wind model can reproduce the vortices triggered by urban buildings well, and that the flow patterns in urban street canyons and building clusters can also be repre-

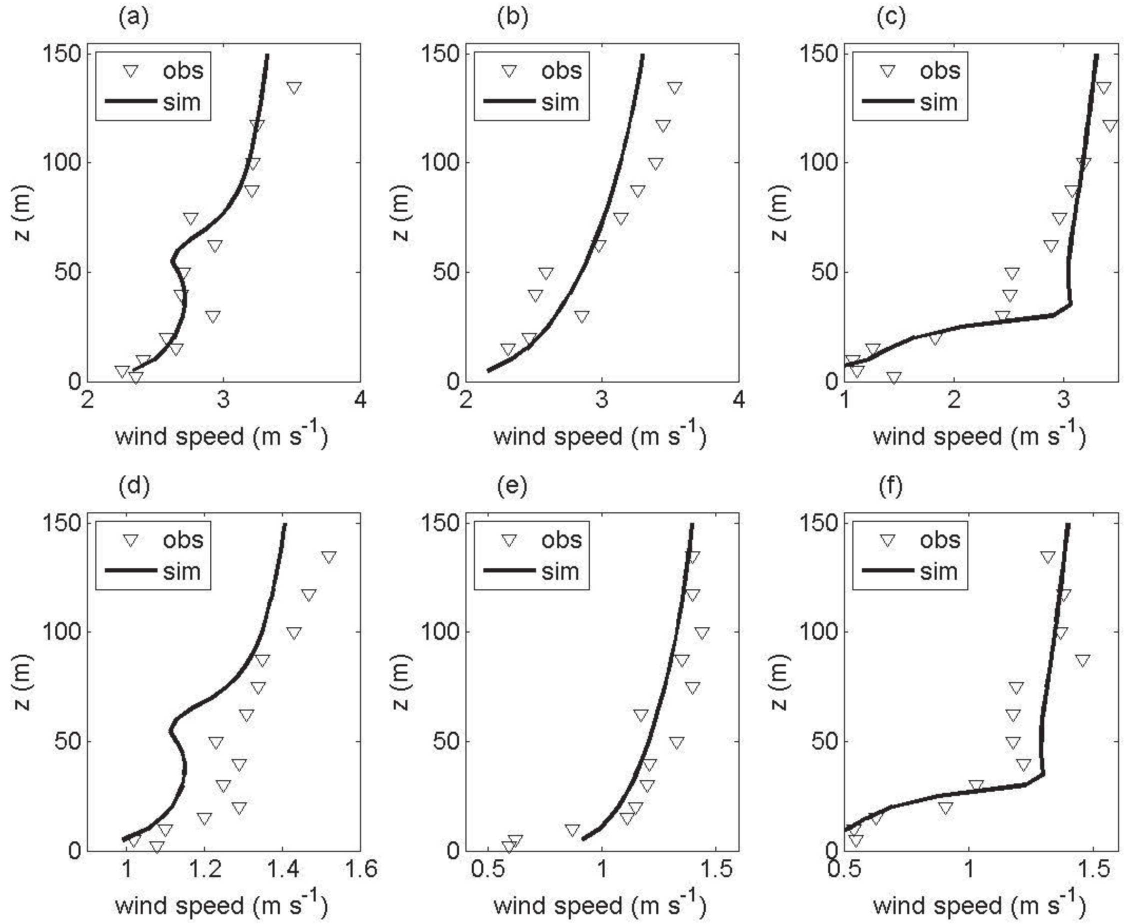

Fig. 7. Observed and simulated vertical profiles of the wind speed in different locations and with different incoming wind speeds with a southwest inlet: (a–c) profiles at locations 1, 2 and 3 for experiments with an incoming wind speed of 1.22 m s^{-1}; (d, e) for experiments with an incoming wind speed of 2 m s^{-1}. Measurements in the wind tunnel experiments are taken at the heights of 2 m, 5 m, 10 m, 15 m, 20 m, 30 m, 40 m, 50 m, 62.5 m, 75 m, 87.5 m, 100 m, 117.5 m and 135 m.

Table 3. Computational efficiencies of different cases.

	Resolution (m) (dx, dy, dz)	Domain size (km) (X, Y, Z)	Grid number (10 000)	Building number	Iteration step number	CPU time (min)
CEDVAL B1-4	(1,1,1)	(0.4,0.2,0.045)	360	4	1281	3.28
	(2,2,1)	(0.4,0.2,0.045)	90	4	702	0.45
FZ-A	(5,5,2)	(1,1,0.2)	400	30	718	1.6
	(10,10,4)	(1,1,0.2)	50	30	1019	0.4
FZ-B	(5,5,2)	(1,1,0.2)	400	30	1500	2.7
	(10,10,4)	(1,1,0.2)	50	30	814	0.3

sented. Due to the complex shapes of buildings and their distributions, the simulation deviations/discrepancies from the measurements are usually caused by the simplification of building shapes and the determination of the key zone sizes and the lack of physical description, because the determination of the key zones is only based on several empirical coefficients mostly estimated from previous wind tunnel studies on regular buildings. The model typically overestimates the horizontal wind speed near street canyon exits, and may also miss the skimming flow vortex behind slanted roofs.

The computational efficiencies of different cases were also discussed in this paper. The model produced very high-resolution (several to ten meters) wind fields on the neighborhood scale (several to ten km) in just minutes. The computational efficiency is affected by the simulation size, model resolution and the iteration loop number in the mass conservation wind model; the building numbers and building shapes have little influence. Given the computational skill, the model could be a strong candidate for prediction and environmental impact evaluation in urban emergency response conditions.

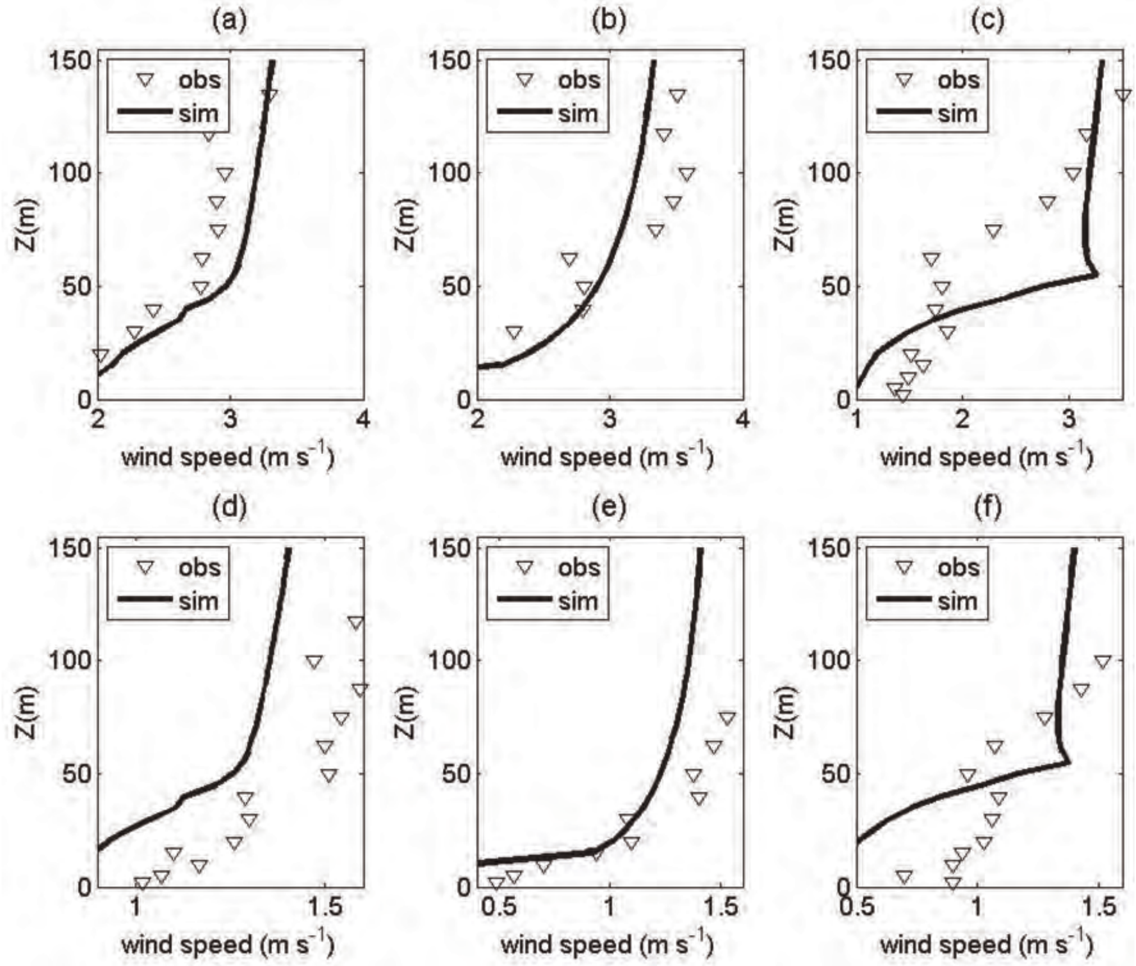

Fig. 8. As in Fig. 7 but for the northwest experiments and the profiles observed at locations 4, 2 and 5.

Acknowledgements. This work was supported by the China Special Fund for Meteorological Research in the Public Interest (Grant No. GYHY201106049), the National Natural Science Foundation of China (Grant Nos. 51538005 and 41375014), and the Jiangsu Collaborative Innovation Center for Climate Change, China.

REFERENCES

Ahmad, K., M. Khare, and K. K. Chaudhry, 2005: Wind tunnel simulation studies on dispersion at urban street canyons and intersections—A review. *Journal of Wind Engineering and Industrial Aerodynamics*, **93**, 697–717.

Arnfield, A. J., 2003: Two decades of urban climate research: A review of turbulence, exchanges of energy and water, and the urban heat island. *Int. J. Climatol.*, **23**, 1–26.

Ashie, Y., and T. Kono, 2011: Urban-scale CFD analysis in support of a climate-sensitive design for the Tokyo Bay area. *Int. J. Climatol.*, **31**, 174–188.

Chang, C. H., J. S. Lin, C. M. Cheng, and Y. S. Hong, 2013: Numerical simulations and wind tunnel studies of pollutant dispersion in the urban street canyons with different height arrangements. *Journal of Marine Science and Technology*, **21**, 119–126.

Claus, J., P. Å. Krogstad, and I. P. Castro, 2012: Some measurements of surface drag in urban-type boundary layers at various wind angles. *Bound.-Layer Meteor.*, **145**, 407–422.

Eliasson, I., B. Offerle, C. S. B. Grimmond, and S. Lindqvist, 2006: Wind fields and turbulence statistics in an urban street canyon. *Atmos. Environ.*, **40**, 1–16.

Fujiwara, C., K. Yamashita, M. Nakanishi, and Y. Fujiyoshi, 2011: Dust devil-like vortices in an urban area detected by a 3D scanning Doppler Lidar. *J. Appl. Meteor. Climatol.*, **50**, 534–547.

Hertwig, D., G. C. Efthimiou, J. G. Bartzis, and B. Leitl, 2012: CFD-RANS model validation of turbulent flow in a semi-idealized urban canopy. *Journal of Wind Engineering and Industrial Aerodynamics*, **111**, 61–72.

Hu, X.-M., M. Xue, P. M. Klein, B. G. Illston, and S. Chen, 2016: Analysis of urban effects in Oklahoma city using a dense surface observing network. *J. Appl. Meteor. Climatol.*, **55**, 723–741, doi: 10.1175/JAMC-D-15-0206.1.

Kochanski, A. K., E. R. Pardyjak, R. Stoll, A. Gowardhan, M. J. Brown, and W. J. Steenburgh, 2015: One-way coupling of the WRF–QUIC urban dispersion modeling system. *J. Appl. Meteor. Climatol.*, **54**, 2119–2139.

Li, X. X., R. E. Britter, T. Y. Koh, L. K. Norford, C. H. Liu, D. Entekhabi, and D. Y. C. Leung, 2010: Large-eddy simulation of flow and pollutant transport in urban street canyons with ground heating. *Bound.-Layer Meteor.*, **137**, 187–204.

Marciotto, E. R., and G. Fisch, 2013: Wind tunnel study of turbulent flow past an urban canyon model. *Environmental Fluid Mechanics*, **13**, 403–416.

Michioka, T., A. Sato, and K. Sada, 2013: Large-eddy simulation coupled to mesoscale meteorological model for gas dispersion in an urban district. *Atmos. Environ.*, **75**, 153–162.

Offerle, B., I. Eliasson, C. S. B. Grimmond, and B. Holmer, 2007: Surface heating in relation to air temperature, wind and turbulence in an urban street canyon. *Bound.-Layer Meteor.*, **122**, 273–292.

Oke, T. R., 1988: Street design and urban canopy layer climate. *Energy and Buildings*, **11**, 103–113.

Ouyang, Y., W. M. Jiang, F. Hu, S. G. Miao, and N. Zhang, 2003: Experimental study in wind tunnel in the field of air flows and pollutant dispersion in the urban sub-domain. *Journal of Nanjing University (Natural Sciences)*, **39**, 770–780. (in Chinese with English abstract)

Rotach M. W., and Coauthors, 2005: BUBBLE-an urban boundary layer meteorology project. *Theor. Appl. Climatol*, **81**, 231-261.

Salem, N. B., V. Garbero, P. Salizzoni, G. Lamaison, and L. Soulhac, 2015: Modelling pollutant dispersion in a street network. *Bound.-Layer Meteor.*, **155**, 157–187.

Singh, B., B. S. Hansen, M. J. Brown, and E. R. Pardyjak, 2008: Evaluation of the QUIC-URB fast response urban wind model for a cubical building array and wide building street canyon. *Environmental Fluid Mechanics*, **8**, 281–312.

Vardoulakis, S., B. E. A. Fisher, K. Pericleous, and N. Gonzalez-Flesca, 2003: Modelling air quality in street canyons: A review. *Atmos. Environ.*, **37**(2), 155–182.

Wood, C. R., L. Pauscher, H. C. Ward, S. Kotthaus, J. F. Barlow, M. Gouvea, S. E. Lane, and C. S. B. Grimmond, 2013: Wind observations above an urban river using a new lidar technique, scintillometry and anemometry. *Science of the Total Environment*, **442**, 527–533.

Wyszogrodzki, A. A., S. G. Miao, and F. Chen, 2012: Evaluation of the coupling between mesoscale-WRF and LES-EULAG models for simulating fine-scale urban dispersion. *Atmos. Res.*, **118**, 324–345.

Xie, Z. T., O. Coceal, and I. P. Castro, 2008: Large-eddy simulation of flows over random urban-like obstacles. *Bound.-Layer Meteor.*, **129**, 1–23.

Zhang, N., W. M. Jiang, and S. G. Miao, 2006: A large eddy simulation on the effect of buildings on urban flows. *Wind and Structures*, **9**, 23–35.

Zhang, N., Y. S. Du, and S. G. Miao, 2016: A microscale model for air pollutant dispersion simulation in urban areas: Presentation of the model and performance over a single building. *Adv. Atmos. Sci.*, **33**, 184–192, doi: 10.1007/s00376-015-5152-1.